# A Graphene and Aptamer Based Liquid Gated FET-Like Electrochemical Biosensor to Detect Adenosine Triphosphate

Souvik Mukherjee, Xenia Meshik, Min Choi, Sidra Farid, Debopam Datta, Yi Lan, Shripriya Poduri, Ketaki Sarkar, Undarmaa Baterdene, Ching-En Huang, Yung Yu Wang, Peter Burke, *Member, IEEE*, Mitra Dutta, *Fellow, IEEE*, and Michael A. Stroscio, *Fellow, IEEE*

***Abstract*—Here we report successful demonstration of a FET-like electrochemical nano-biosensor to accurately detect ultralow concentrations of adenosine triphosphate. As a 2D material, graphene is a promising candidate due to its large surface area, biocompatibility, and demonstrated surface binding chemistries and has been employed as the conducting channel. A short 20-base DNA aptamer is used as the sensing element to ensure that the interaction between the analyte and the aptamer occurs within the Debye length of the electrolyte (PBS). Significant increase in the drain current with progressive addition of ATP is observed whereas for control experiments, no distinct change in the drain current occurs. The sensor is found to be highly sensitive in the nanomolar (nM) to micromolar ($\mu$M) range with a high sensitivity of 2.55 $\mu\mathrm{A}\ (\mathrm{mM})^{-1}$, a detection limit as low as 10 pM, and it has potential application in medical and biological settings to detect low traces of ATP. This simplistic design strategy can be further extended to efficiently detect a broad range of other target analytes.**

***Index Terms*—Adenosine triphosphate, atomic force microscopy, DNA aptamer, electrochemical detection, graphene field effect transistor.**

## I. Introduction

ADENOSINE triphosphate (ATP) is present in all living cells and provides energy for a wide variety of cellular processes. Each molecule of ATP contains three phosphate groups where potential energy is stored and released upon the phosphate group's removal. Phosphorylation and dephosphorylation of ATP are continuously occurring processes in cells, as energy is needed constantly to maintain the cell's metabolism. It is estimated that the body turns over its own weight equivalent of ATP each day [1]. Detecting ATP is therefore of great importance in various biological fields, and so far many methods have been developed to detect ATP concentrations [2]–[4].

Due to an unprecedented growth in the area of device fabrication and processing, researchers have been able to successfully achieve devices in the nanoscale dimension with high precision and reliability, which are comparable in size with biological structures and have paved the way in their integration. The choice of using field effect transistors (FETs) for biosensing applications is not new and over the years researchers have considered FET-like structures mainly due to the ease of manufacturing using standard device processing techniques, real-time detection, cheap and label free detection of biomolecules, low-level detection capability, low power consumption and possibility of integration on a chip [5]–[8]. Stroscio *et al.* [9] demonstrated potential application, developments, and impact of integrated biological-semiconductor devices. The term FET-like is being used to point out the subtle difference between a traditional FET and liquid gated FET which is reported in this paper.

Aptamers are functional single-stranded DNA or RNA molecules selected *in vitro* to bind to a specific target analyte including metal ions [6], [10], [11] such as $\mathrm{Pb}^{2+}$, $\mathrm{K}^{+}$, $\mathrm{UO}_2^{2+}$; organic and inorganic molecules [12] and proteins [13]. Aptamers have been widely used as sensing element in biosensors and have emerged as a potential alternative to natural receptors like antibody-based immunoassays due to several advantages including ease of synthesis and regeneration over antibodies, high chemical and thermal stability, small size and wide range of target binding ability [12], [14].

In recent years, there has been an increasing trend of aptamer-based biosensing based on using 1D and 2D nanomaterials as channel components [15], [16] but there remains associated challenges and need for further exploration to design biosensors with high sensitivity, selectivity and lower detection limit. 1D nanomaterials like nanowires and single walled carbon nanotubes (SWNTs) offer several advantages including high sensitivity in comparison to their bulk counterparts, size compatibility, and also biocompatibility [7]. However, the main disadvantage of using 1D material is that their synthesis and integration process is not so typical and requires sophisticated

Manuscript received September 28, 2015; accepted November 07, 2015. This work was supported in part, by Army Research Office (ARO) through the MURI Grant No. W911NF-11-1-0024. Date of publication November 18, 2015; date of current version January 07, 2016. *Asterisk indicates corresponding author.*

S. Mukherjee, M. Choi, S. Farid, D. Datta, Y. Lan, S. Poduri, K. Sarkar, C.-E. Huang, M. Dutta, and M. A. Stroscio are with the Electrical and Computer Engineering Department, University of Illinois at Chicago, Chicago, IL 60607 USA (e-mail: smukhe8@uic.edu; mchoi29@uic.edu; sfarid3@uic.edu; ddatta2@uic.edu; ylan3@uic.edu; spodur2@uic.edu; ksarka3@uic.edu; chingenhuang@gmail.com; dutta@uic.edu; stroscio@uic.edu).

X. Meshik, and U. Baterdene are with the Bioengineering Department, University of Illinois at Chicago, Chicago, IL 60607 USA (e-mail: xmeshi2@uic.edu; ubater2@uic.edu).

Y. Y. Wang is with the Chemical Engineering and Materials Science Department, University of California Irvine, Irvine, CA 92697 USA (e-mail: willwang107@gmail.com).

P. Burke is with the Electrical Engineering and Computer Science Department, University of California Irvine, Irvine, CA 92697 USA (e-mail: pburke@uci.edu).

Color versions of one or more of the figures in this paper are available online at http://ieeexplore.ieee.org.

Digital Object Identifier 10.1109/TNB.2015.2501364

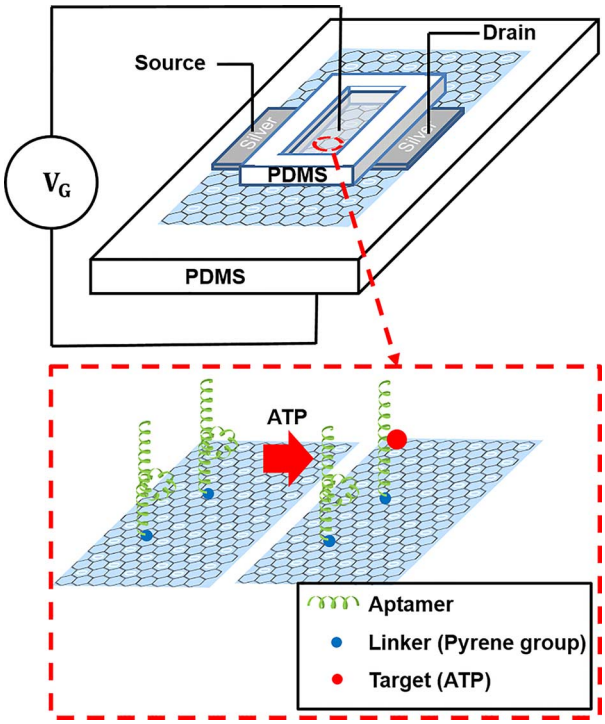


Fig. 1. Schematic representation of liquid gated FET-like aptamer-based biosensor with a single layer of graphene deposited on a PDMS substrate acting as the conducting channel; silver paste serves as contacts for both source and drain. Inset showing the immobilized aptamers with a 5' pyrene modification attached to the graphene layer *via* $\pi$-$\pi$ stacking undergoing conformational change upon addition of ATP.

fabrication techniques to realize them. This is one of the reasons that have impaired their use in practical applications. As a result, 2D materials like graphene [5], [6], [17], [18] and $MoS_2$ [15] have gained much attention and are being extensively investigated as an alternative to 1D structures to form the channel component. Graphene is of particular interest in biosensing due to its 2D structure, biocompatibility and effective ligand surface binding chemistries and as a result, has been considered in this aptamer-based work. There are different approaches to design aptamer-based label free biosensors which can be classified as electrochemical [5], [17], optical [19]–[21] and mass-sensitive [22], [23], based on their detection methodology. Here we report a label free aptamer-based electrochemical biosensor employing monolayer graphene as the conducting channel to detect adenosine triphosphate. Fig. 1 shows a schematic representation of the liquid gated FET-like aptamer-based biosensor.

## II. Experimental Details

### A. Fabrication of Graphene FET Like Structures

Graphene FET-like devices were fabricated at the University of California at Irvine using previously-described protocols [5]. Briefly, graphene was grown on copper foil via low pressure chemical vapor deposition and transferred onto a polydimethylsiloxane (PDMS) layer. Raman investigation was performed to verify monolayer properties of graphene [24] and indicate any defects [25] caused during transfer-printing. A rectangular hollow PDMS piece was then placed on top, forming a well with a graphene layer on the bottom and PDMS on the sides. Source and drain terminals were created by coating the edges of the graphene surface outside the well with colloidal silver paste (Ted Pella, Redding, CA, USA).

### B. Aptamer Immobilization on Graphene Surface

A stock solution of 75 $\mu$M aptamer was diluted to 15 $\mu$M in anhydrous dimethylformamide (DMF) (Sigma Aldrich, St. Louis, MO, USA). A 50-$\mu$L drop of aptamer solution was placed into the well of the FET-like structure and left for 2 h at room temperature. The well was then washed three times with phosphate buffered saline (PBS) to remove any unattached aptamers and filled with 50 $\mu$L of PBS. For control purposes, separate wells were prepared with no aptamer present to confirm that the aptamer-ATP binding was in fact the cause of any changes in device transfer curves.

### C. Electrochemical Detection of ATP

Ag/AgCl gate electrode (Microelectrodes, Inc., Bedford, NH, USA) filled with 3 M KCl was placed into the PBS inside the well. Gate voltages of $-0.8$ V to 0.8 V were applied and source-drain current measurements were carried out using an Agilent semiconductor parameter analyzer. ATP (Sigma Aldrich, St. Louis, MO) was dissolved in PBS and various concentrations in the range of 0.1 pM to 1 mM were added to the well, at which point device transfer curves were obtained. Aside from the control experiments with no aptamer present, additional control experiments were performed in which the amino acid L-cysteine (Sigma Aldrich, St. Louis, MO, USA) was added to the aptamer-functionalized device instead of ATP. While any non-target molecule would serve the purpose, L-cysteine is comparable in size to ATP, making it more suitable for control experiments.

## III. Results and Discussion

### A. Favorable Conformations and Analytical Selection of ATP Aptamer

ATP aptamer sequence was chosen based on previously published work by Huizenga *et al.* and Li *et al.* (Table I) [26], [27]. The aptamers used in these studies all contain a common 20-base motif, suggesting that it is the key binding site of ATP [27], [28]. Since our study requires the aptamer and ATP binding to occur as close as possible to the graphene surface so as to not exceed the Debye length of the electrolyte, the shortest aptamer sequence is preferable. Therefore, the 20-base sequence 5'-/Pyrene/GGGGGAGTATTGCGGAGGAA-3' from Biosearch Technologies (Novato, CA, USA) was used. The favorable conformations based on the lowest folding energies are shown in Fig. 2 obtained using the Mfold software. The 5' pyrene group serves to bind the aptamer to the graphene, since the benzene rings on the pyrene group interact with the graphene *via* $\pi$-$\pi$ stacking.

### B. AFM Technique for Structural Verification of DNA Aptamer-Graphene Binding

There are different detection techniques that are used to verify the immobilization of the DNA aptamer on the graphene surface. Optical detection using fluorescent quantum dot tagged

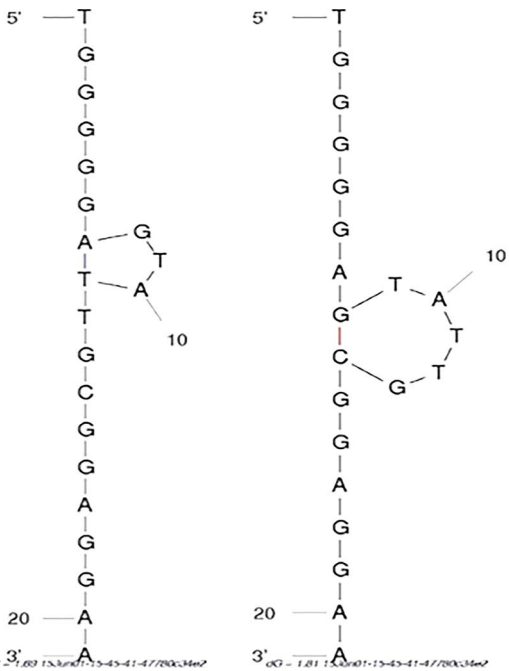


Fig. 2. Most probable conformations of ATP aptamer selected for this study, produced using Mfold software.

TABLE I
SEQUENCES OF ATP APTAMERS USED IN PREVIOUSLY-PUBLISHED STUDIES. THE HIGHLIGHTED MOTIF WAS CONSISTENT IN TWO OF THE APTAMERS AND WAS THEREFORE USED IN THIS STUDY

| No. | Aptamer sequence (5' to 3') | Reference |
|---|---|---|
| 1 | GTG CT***T GGG GGA GTA TTG CGG AGG AA***A GCG GCC CTG CTG AAG | Huizenga et al., 1995 |
| 2 | GGG UUG GGA AGA AAC UGU GGC ACU UCG GUG CCA GCA ACC C | Sassanfar et al., 1993 |
| 3 | GCA CC***T GGG GGA GTA TTG CGG AGG AA***G GT | Li et al., 2012 |

aptamer is a common method to verify the binding [6]. Instead we report a further simpler technique using atomic force microscopy (AFM). 15 $\mu$M solution of the aptamer was prepared and 10 $\mu$L was drop casted on one side of the graphene surface and was left overnight. No aptamer was dropped on the other side of the graphene surface. The sample was washed thoroughly for 12 h to remove any unbound aptamers and impurities from the surface. AFM measurements were performed using Bruker ICON Dimension system as shown in Fig. 3. The aptamer attached regions shows structures of height around 20–50 nm assumed to be originating due to coalescing of aptamers binding to the graphene surface whereas the no aptamer region does not have any distinguishable structures. Non-uniform surface appearing in the no aptamer region is believed to be originating due to the surface roughness of the PDMS substrate. To verify reproducibility, measurements were performed on multiple samples following the exact same procedure.

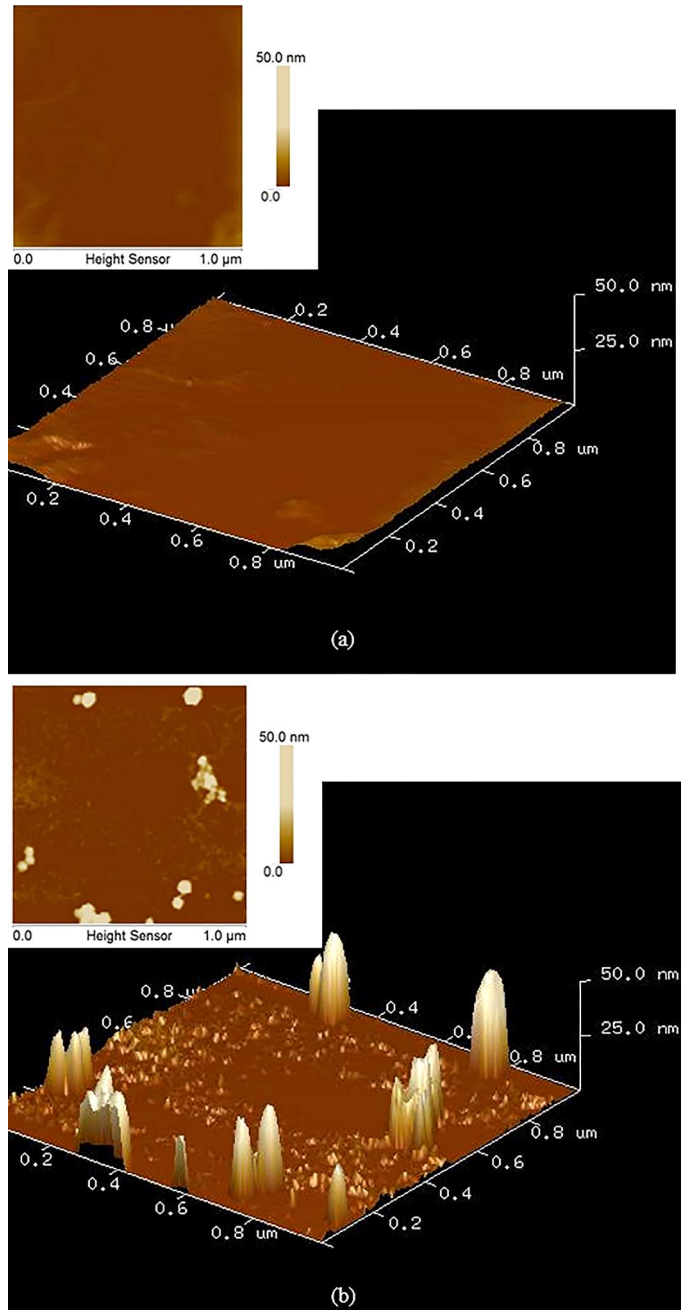


Fig. 3. (a) AFM images showing no aptamer region and (b) cluster of aptamers on the graphene surface scanned over an area of 1 $\mu$m by 1 $\mu$m. Inset of plots shows corresponding 2D profile.

### *C. Graphene FET Device Characteristics and Detection Mechanism*

The device transfer characteristics (drain current $I_d$ vs. gate voltage $V_g$) measured using HP 4156B parameter analyzer, exhibit ambipolar field effect characteristics as shown in Fig. 4. The relative change in the $I_d$ is measured at the minimum conductance point of the transfer curve also known as the Dirac point. The measurements have been repeated over different samples and the Dirac point is found to be shifted from the origin to a small positive voltage range (0.2–0.4 V). This shift is assumed to be occurring due to unintentional p-type doping from deionized water and also due to impurities incorporated

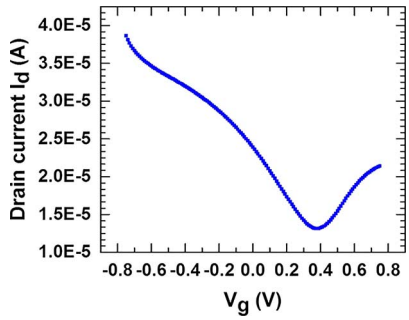


Fig. 4. Transfer characteristics of the sensor at constant $V_{DS} = 0.3$ V.

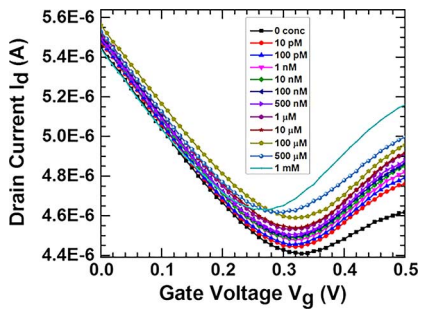


Fig. 5. $I_d$-$V_g$ transfer characteristics of the FET-like sensor with varied ATP concentrations progressively added in the presence of aptamer.

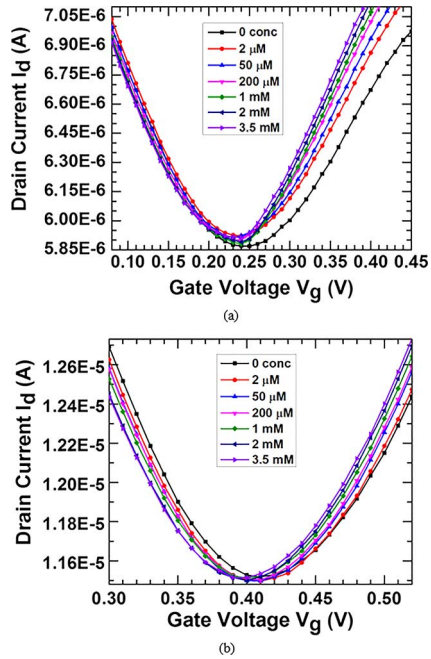


Fig. 6. Control experiments showing $I_d$-$V_g$ transfer characteristics of the FET-like sensor (a) ATP without aptamer present and (b) L-cysteine with the aptamer present.

on or underneath the graphene surface during the fabrication process [29], [30]. The $I_d$ at corresponding $V_{Dirac}$ points for different samples are found to be within the range 4.4–13.5 $\mu$A as the current depends on the properties of the graphene surfaces.

An in depth analysis is necessary to clearly understand the underlying mechanism of the graphene based biosensor. The quality of the graphene layer and the length of aptamer sequence being used are two important factors that determine the response of the sensor. Due to ambipolar characteristics of graphene, the device transfer curve is assumed to have two separate sections across the Dirac point occurring due to the formation of two different conduction channels depending on the channel carrier density as a function of the applied gate voltage. $I_d$ is found to be increasing on the right side of the Dirac point indicating an n-type channel formation due to accumulation of electrons at a higher gate voltage. The left side of the Dirac point indicates a p-type region due to formation of channel with holes as majority carriers.

Fig. 5 shows the $I_d$-$V_g$ plot with aptamer and ATP target concentration added progressively from 0 pM to 1 mM. The gate voltage $V_g$ is varied from $-0.8$ V to 0.8 V and the source-drain voltage is maintained constant at 0.3 V.

Due to short aptamer structure which is inside the Debye length of the electrolyte [31], reaction occurs between the target and the aptamer resulting in conformational change in the aptamer structure and the change is reflected in the charge distribution in the electrolyte on the graphene layer. As determined experimentally, the current, $I_d$, at the Dirac point is found to be increasing with increasing target concentration. $V_{Dirac}$ point also decreases and experiences a negative shift indicating an n-type doping effect introduced due to charge carriers. The percentage change in current after adding ATP has been used to indicate the detection mechanism in this paper. The results are in agreement with previous studies by Zuo *et al.* [32] which reported an aptamer-based target-responsive electrochemical switch where the peak current increased with increase in the aptamer concentration; Li *et al.* [19] reported detection based on change in the resonance energy transfer.

### *D. Selectivity, Sensitivity, and Detection Limit of ATP Electrochemical Sensor*

To test the selectivity of the sensor, control experiments were performed with no aptamer attached to the graphene surface and L-cysteine as the target analyte as shown in Fig. 6. The lack of response from both control experiments relative to the ATP with aptamer experiments where we observe a significant increase in the $I_d$ at Dirac point, helps us to conclude the successful detection of ATP. It can be also seen from both the control experiments that there is no significant shift in the $V_{Dirac}$ point indicating no doping effect which proves there is no change in the surface charge distribution and hence the biosensor is non receptive to other targets.

A nonlinear trend line as shown in Fig. 7(a) is used to obtain a fit with the $I_d$ data measured at the Dirac point following the exponential decay model which shows strong correlation ($R^2 = 0.96$). The normalized relative percentage change in $I_d$ while the target concentration is varied from 0 pM–1 mM is plotted in Fig. 7(b). The sensitivity of the sensor is calculated by taking the first order derivative of the nonlinear trendline equation, as in (1) and is found to be $\sim 2.55\ \mu\text{A}(\text{mM})^{-1}$ within the

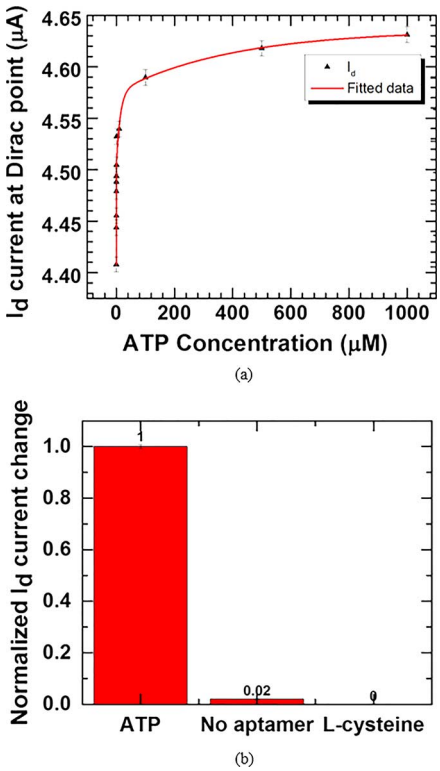


Fig. 7. (a) Selectivity of the sensor calculated based on normalized percentage change in the $I_d$ due to variation in target concentration from 0 pM–1 mM at the Dirac point and (b) change in $I_d$ obtained due to change in the ATP concentration and fitted with a nonlinear trend line following the exponential decay model.

range 0 pM–50 $\mu$M where x is the concentration value expressed in micromolar ($\mu$M).

$$I_{\text{Dirac}} = -0.09657e^{-x/7.54857e^{-4}} + 0.07072e^{-x/13.1241} + 0.06045e^{-x/397.31692} + 4.63573. \quad (1)$$

It is seen that the sensor's ability to detect any current change starts to saturate after 100 $\mu$M target concentration, which can be considered as an upper bound. The upper detection limit is bound due to the device structure where the dimensions of the well containing the electrolyte is roughly (0.8 cm $\times$ 0.4 cm $\times$ 0.2 cm) and is designed mainly to detect ultralow concentrations.

The traditional method of approximating the lower bound of detection (LOD) by dividing resolution by sensitivity fails to apply in this case as our sensor is non-reusable in nature and one needs to perform repeated measurements to calculate the resolution [33]. In order to analyze the lower detection limit of the proposed sensor, target concentration has been added as low as 1 pM and the response of the sensor is recorded. The lowest target concentration detected was between 1 pM and 10 pM due to the instrumental limitation determined from the resolution of the HP 4156B parameter analyzer which is found to be $\sim$ 10 pA in the measurement range of this work.

## IV. Conclusion

In this work, we have reported a unique liquid gated FET-like nanobiosensor and proved its effectiveness to successfully determine ultralow concentration of ATP target analytes. Several advantages of the sensor include label free detection, simplistic design, stability, high selectivity and sensitivity, and low concentration detection capability. Our sensor based on electrochemical sensing shows comparable and better response than previously reported strategies employing FRET [19], [20], [34]; TREAS [32] or nanoparticle based ATBR [35] to detect ATP. Comparable to our sensor performance, only a few investigators—including Li *et al.*—have previously reported detection limit of 0.01 nM and operating range within 0.1 nM–1 $\mu$M. Others [20], [32], [34], [35] have reported operating range and detection limit primarily in the millimolar (mM) range and our sensor outperforms them by a significant margin and thus offers a new direction for low power, high performance electrochemical sensing of a wide range of target analytes based on nanoscale graphene platform.

## Acknowledgment

The authors would like to thank the Nanotechnology Core Facility (NCF) at University of Illinois at Chicago for providing clean room facilities to perform various measurements.

## References

[1] S. Törnroth-Horsefield and N. Richard, "Opening and closing the metabolite gate," *Proc. Natl. Acad. Sci.*, vol. 105, no. 50, pp. 19565–19566, Dec. 2008.

[2] P. Held, "Fluorimetric quantitation of protein using the reactive compound fluorescamine," BioTek Instrum., Winooski, VT, USA, 2006 [Online]. Available: http://www.nature.com/app_notes/nmeth/2006/063006/full/an1794.html

[3] M. Helenius, S. Jalkanen, and G. G. Yegutkin, "Enzyme-coupled assays for simultaneous detection of nanomolar ATP, ADP, AMP, adenosine, inosine and pyrophosphate concentrations in extracellular fluids," *BBA-Mol. Cell Res.*, vol. 1823, no. 10, pp. 1967–1975, Oct. 2012.

[4] S. W. Schneider, M. E. Egan, B. P. Jena, W. B. Guggino, H. Oberleithner, and J. P. Geibel, "Continuous detection of extracellular ATP on living cells by using atomic force microscopy," *Proc. Natl. Acad. Sci.*, vol. 96, no. 21, pp. 12180–12185, Oct. 1999.

[5] Y. Y. Wang and P. J. Burke, "A large-area and contamination-free graphene transistor for liquid-gated sensing applications," *Appl. Phys. Lett.*, vol. 103, no. 5, pp. 052103-1–052103-4, Jul. 2013.

[6] K. Xu, X. Meshik, B. M. Nichols, E. Zakar, M. Dutta, and M. A. Stroscio, "Graphene-and aptamer-based electrochemical biosensor," *Nanotechnology*, vol. 25, no. 20, p. 205501, Apr. 2014.

[7] J. Kim, Y. S. Rim, H. Chen, H. H. Cao, N. Nakatsuka, H. L. Hinton, C. Zhao, A. M. Andrews, Y. Yang, and P. S. Weiss, "Fabrication of high-performance ultrathin In2O3 film field-effect transistors and biosensors using chemical lift-off lithography," *ACS Nano*, vol. 9, no. 4, pp. 4572–4582, Apr. 2015.

[8] S. Liu and X. Guo, "Carbon nanomaterials field-effect-transistor-based biosensors," *NPG Asia Mater.*, vol. 4, no. e23, pp. 1–9, Aug. 2012.

[9] M. A. Stroscio and M. Dutta, "Integrated biological-semiconductor devices," *Proc. IEEE*, vol. 93, no. 10, pp. 1772–1783, Oct. 2005.

[10] Z. Jiang, Y. Zhang, A. Liang, C. Chen, J. Tian, and T. Li, "Free-labeled nanogold catalytic detection of trace UO 2 2+ based on the aptamer reaction and gold particle resonance scattering effect," *Plasmonics*, vol. 7, no. 2, pp. 185–190, Jun. 2012.

[11] K. L. Brenneman, S. Poduri, M. A. Stroscio, and M. Dutta, "Optical detection of lead (II) ions using DNA-based nanosensor," *IEEE Sensors J.*, vol. 13, no. 5, pp. 1783–1786, Jan. 2013.

[12] H. Zhang, B. Jiang, Y. Xiang, Y. Zhang, Y. Chai, and R. Yuan, "Aptamer/quantum dot-based simultaneous electrochemical detection of multiple small molecules," *Anal. Chim. Acta.*, vol. 688, no. 2, pp. 99–103, Mar. 2011.

[13] N. Hamaguchi, A. Ellington, and M. Stanton, "Aptamer beacons for the direct detection of proteins," *Anal. Biochem.*, vol. 294, no. 2, pp. 126–131, Jul. 2011.

[14] J. Zhao, C. Chen, L. Zhang, J. Jiang, and R. Yu, "An electrochemical aptasensor based on hybridization chain reaction with enzyme-signal amplification for interferon-gamma detection," *Biosens. Bioelectron.*, vol. 36, no. 1, pp. 129–134, Jun.–Jul. 2012.

[15] D. Sarkar, W. Liu, X. Xie, A. C. Anselmo, S. Mitragotri, and K. Banerjee, "MoS2 field-effect transistor for next-generation label-free biosensors," *ACS Nano*, vol. 8, no. 4, pp. 3992–4003, Mar. 2014.
[16] B. L. Allen, P. D. Kichambare, and A. Star, "Carbon nanotube field-effect-transistor-based biosensors," *Adv. Mater.*, vol. 19, no. 11, pp. 1439–1451, Apr. 2007.
[17] S. Farid, X. Meshik, M. Choi, S. Mukherjee, Y. Lan, D. Parikh, S. Poduri, U. Baterdene, C. Huang, Y. Y. Wang, P. Burke, M. Dutta, and M. A. Stroscio, "Detection of Interferon gamma using graphene and aptamer based FET-like electrochemical biosensor," *Biosens. Bioelectron.*, vol. 71, pp. 294–299, Sep. 2015.
[18] K. Xu, M. Purahmad, K. Brenneman, X. Meshik, S. Farid, S. Poduri, P. Pratap, J. Abell, Y. Zhao, B. Nichols, E. Zakar, M. A. Stroscio, and M. Dutta*, Design and Applications of Nanomaterials for Sensors*, ser. Challenges and Advances in Computational Chemistry and Physics, J. M. Seminario, Ed., 1st ed. Dordrecht, The Netherlands: Springer, 2014, vol. 16, pp. 61–97.
[19] Z. Li, Y. Wang, Y. Liu, Y. Zeng, A. Huang, N. Peng, X. Liu, and J. Liu, "A novel aptasensor for the ultra-sensitive detection of adenosine triphosphate via aptamer/quantum dot based resonance energy transfer," *Analyst*, vol. 138, no. 17, pp. 4732–4736, Sep. 2013.
[20] Z. Chen, G. Li, L. Zhang, J. Jiang, Z. Li, Z. Peng, and L. Deng, "A new method for the detection of ATP using a quantum-dot-tagged aptamer," *Anal. Bioanal. Chem.*, vol. 392, no. 6, pp. 1185–1188, Nov. 2008.
[21] K. L. Brenneman, B. Sen, M. A. Stroscio, and M. Dutta, "Aptamer-based optical bionano sensor for mercury (II) ions," in *Proc. IEEE NMDC*, 2010, pp. 221–224.
[22] A. Janshoff, H. J. Galla, and C. Steinem, "Piezoelectric mass-sensing devices as biosensors—An alternative to optical biosensors?," *Angew. Chem. Int. Ed*, vol. 39, no. 22, pp. 4004–4032, Nov. 2000.
[23] R. Raiteri, M. Grattarola, H. J. Butt, and P. Skládal, "Micromechanical cantilever-based biosensors," *Sensor Actuat. B, Chem.*, vol. 79, no. 2–3, pp. 115–126, Nov. 2001.
[24] D. Graf, F. Molitor, K. Ensslin, C. Stampfer, A. Jungen, C. Hierold, and L. Wirtz, "Spatially resolved Raman spectroscopy of single-and few-layer graphene," *Nano Lett.*, vol. 7, no. 2, pp. 238–242, Jan. 2007.
[25] S. Farid, S. Mukherjee, H. Jung, M. A. Stroscio, and M. Dutta, "Analysis on the structural, vibrational and defect states of chlorine treated polycrystalline cadmium telluride structures grown by e-beam evaporation," *Mater. Res. Exp.*, vol. 2, no. 2, p. 025007, Feb. 2015.
[26] D. E. Huizenga and J. W. Szostak, "A DNA aptamer that binds adenosine and ATP," *Biochemistry*, vol. 34, no. 2, pp. 656–665, Jan. 1995.
[27] M. Li, J. Zhang, S. Suri, L. J. Sooter, D. Ma, and N. Wu, "Detection of adenosine triphosphate with an aptamer biosensor based on surface-enhanced Raman scattering," *Anal. Chem.*, vol. 84, no. 6, pp. 656–665, Feb. 2012.
[28] M. Sassanfar and J. W. Szostak, "An RNA motif that binds ATP," *Nature*, vol. 364, pp. 550–553, Aug. 1993.
[29] K. S. Novoselov, A. K. Geim, S. V. Morozov, D. Jiang, Y. Zhang, S. V. Dubonos, I. V. Grigorieva, and A. A. Firsov, "A. Electric field effect in atomically thin carbon films," *Science*, vol. 306, no. 5696, pp. 666–669, Oct. 2004.
[30] I. Meric, M. Y. Han, A. F. Young, B. Ozyilmaz, P. Kim, and K. L. Shepard, "Current saturation in zero-bandgap, top-gated graphene field-effect transistors," *Nature Nanotechnol.*, vol. 3, pp. 654–659, Sep. 2008.
[31] Y. Ohno, K. Maehashi, and K. Matsumoto, "Label-free biosensors based on aptamer-modified graphene field-effect transistors," *J. Amer. Chem. Soc.*, vol. 132, no. 51, pp. 18012–18013, Dec. 2010.
[32] X. Zuo, S. Song, J. Zhang, D. Pan, L. Wang, and C. Fan, "A target-responsive electrochemical aptamer switch (TREAS) for reagentless detection of nanomolar ATP," *J. Amer. Chem. Soc.*, vol. 129, no. 5, pp. 1042–1043, Jan. 2007.
[33] H. P. Loock and P. D. Wentzell, "Detection limits of chemical sensors: Applications and misapplications," *Sensor Actuat. B, Chem.*, vol. 173, pp. 157–163, Jan. 2012.
[34] Y. Wang and B. Liu, "ATP detection using a label-free DNA aptamer and a cationic tetrahedralfluorene," *Analyst*, vol. 133, no. 11, pp. 1593–1598, Nov. 2008.
[35] J. Wang, L. Wang, X. Liu, Z. Liang, S. Song, W. Li, G. Li, and C. Fan, "A gold nanoparticle-based aptamer target binding readout for ATP assay," *Adv. Mater.*, vol. 19, no. 22, pp. 3943–3946, Nov. 2007.